Journal of New Technology and Materials
(JNTM)
J. New Technol. Mater.
Vol. 11, N°02 (2021)53-57

OEB Univ. Publish. Co.

A simple synthesis of CuO NPs for photocatalytic applications and theirs structural and optical properties.

S. Roguai* and A. Djelloul

Laboratory of Structures, Properties and Interatomic Interactions (LASPI2A), Department of Matter Sciences, Faculty of Sciences and Technology, Abbes Laghrour University Khenchela, 40000,

*Corresponding author, email: rog.sabrina@yahoo.fr
Received date: Aug. 06, 2021 ; accepted date: Oct. 24, 2021

Abstract

In this study, the copper nanoparticles were synthesized by simple co-precipitation method which were obtained by heating at 80°C for photocatalytic application. The microstructural characterization of the nanopowder obtained was performed using X-ray diffraction (XRD), SEM, EDS, and Infrared Spectroscopy (IR). The optical properties of nanoparticles were studied by UV-Visible spectroscopy. XRD studies demonstrated that the formation of CuO monoclinic phase and the average grain size of CuO crystallite were found to be 30 nm. The FTIR spectral analysis showed the characteristics peaks of Cu-O bond. The EDAX result indicated that there were no other elemental impurities present in the prepared CuO nanoparticles. SEM images indicate the morphology as a three-dimensional flower-like structure was successfully prepared for subsequent degradation of methylene blue (MB). With regard to the optical proprieties, the value of the bandgap energy equals 1.34 eV.

Keywords: CuO NPs; X-ray diffraction; SEM; FTIR; and Optical properties; Photocatalytic.

1. Introduction

In recent years, transition metal oxides (TMOs) have attracted considerable interest due to their potential applications such as supercapacitors, sensors, solar cells, photocatalysis and electrochromic devices [1-6]. Among them, Copper nanoparticles and copper oxide with these two stable forms precisely: tenorite (CuO) and cuprite (Cu2O) with band gaps of 1.2-1.9 eV and 2.0-2.2 eV respectively have aroused a great interest in the scientific community worldwide [7, 8]. These two oxides have a p-type semiconductor character due to the presence of copper gaps in their crystallographic structure. These oxides have three main advantages which are : (i) low cost, (ii) less toxicity, (iii) high stability [9-14].

The CuO NPs have different morphologies such as: nanoflowers, nanowires, hollow spheres and octahedra nanorods [15-17], in addition to its crystalline/amorphous nanoparticles facilitates the separation of electron-hole pairs offering an electron transfer surface[18]. Due to their direct electron channels and efficient electron-hole separation during the photocatalytic process, they have attracted a considerable attention in photocatalytic applications[19].

There were many studies about the photocatalytic removal of methylene violet and methylene blue in the presence of CuO nanoparticles wich were prepared by hydrothermally [20]. It was found that CuO nanoparticles reduced by 96% and 89% of methylene violet and methylene blue respectivly dye in 180 minutes [21]. Other studies demensteated the photocatalytic efficiency to remove methylene blue and methylene orange dyes by flower-like CuO microspheres through the reflux condensation technique[15-17].

Several methods are used to synthesize copper oxide nanoparticles such as thermal deposition, electrodeposition, reactive sputtering, microwave-assisted route, facile wet chemical and hydrothermal routes [22-24]. Among these methods, is the co- precipitation chemical method which is simple, economical and allows to obtain large scale nanostructures for many semiconductor nanoparticles.

In this study, copper oxide nanoparticles were obtained by co- precipitation method. These nanoparticles were studied by different characterization techniques such as: X-ray diffraction, SEM scanning electron microscopy, energy-dispersive X-ray spectroscopy (EDX), UV-vis spectroscopy and infrared absorption spectroscopy. The manufacturing of CuO NPs was conducted to investigate the photocatalytic degradation of MB.

2. Experimental section

2.1. Preparation of CuO nanoparticles

CuO NP is obtained by an easy chemical co-precipitation method, a very simple process whose low-temperature synthesis parameters and reduced costs make it the preferred choice compared to other techniques [25], was obtained by the interaction of ammonia with the sulfate solution.

In this experiment, 1.95 g of CuSO4-5H2O was dissolved completely in 100 ml of deionized water. Then, a solution of NH3-H2O (64 ml, 0.26 M) was added rapidly to the CuSO4 solution and stirred for 30 minutes, and then a solution of NaOH (24 ml, 1.4 M) was added at a flow rate of 2 ml/min, controlling the reaction temperature in a water bath at 80 °C. Finally, the CuO

samples were collected, cleaned with deionized water and dehydrated at room temperature.

2.2. Characterization Techniques

The crystalline phases of the as-synthesized CuO NPs were characterized by X-ray diffractometry (XRD) (MiniFlex600) with a monochromatizes Cu Kα irradiation (λ = 0.15418 nm). The surface morphologies and composition analysis were examined by scanning electron microscopy (SEM) and energy-dispersive X-ray spectroscopy (EDX) using a (TESCAN_VEGA3). The FTIR spectra were recorded using Thermo-Nicolet equipment in the 4000-400 cm-1 region. UV-Vis spectra were recorded by a SpectroScan 80D spectrophotometer UV-vis in the 190-1100 nm spectral range. During the photocatalytic experiment, UV-Vis spectroscopy was employed for obtaining the absorption spectra of obtained CuO NPs and examination of photocatalytic activities of *prepared CuO NPs.*

2.3. Photocatalytic experiments

Photocatalytic analyses on synthesized CuO NPs were performed by examining MB decomposition under visible light irradiation. The photochemical reactor consists of an open wooden box, a magnetic rod stirrer and a 10 ml MB solution beaker with a Philips germicidal lamp (G15T8/15W) emitting mainly at 254 nm, with a gap of 7 cm between the lamp and the beaker. 0.002g of CuO NPs was added to the (10ml, 2×10^{-5}M) of MB solution and dispersed by ultrasound for 10 min. Magnetic stirring in the dark for 30 minutes to achieve an MB adsorption-desorption stability on the catalyst surface pretreated the solutions. Afterwards, the solutions were exposed to radiation every 30 minutes and the MB concentration was measured by detecting variations in the highest absorption band (664 nm) of methylene blue (MB) with the Parkin Elmer UV-VIS-NIR Lambda 19 spectrophotometer.

3. Results and discussion

3.1. Structure analysis

The X-ray diffraction spectrum of CuO powder processed at room temperature is shown in Fig. 1. From the X-ray diffraction spectra a good resolution of the peaks can be observed which shows the good quality of the crystallites for CuO powder. From the X-ray diffraction spectra it can be deduced that the prepared CuO powder has a monoclinic phase with symmetry of the group of space (C2/c.), and this by comparison with the database (ASTM sheet N°01-074-1021).

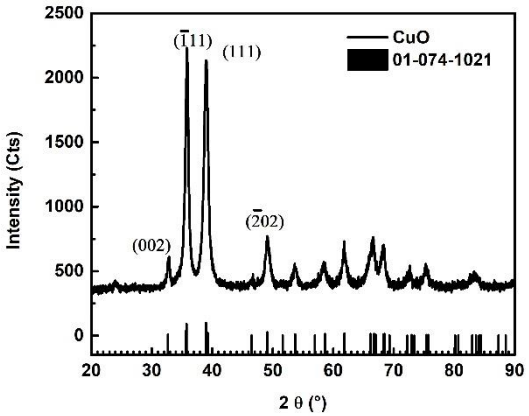

Figure 1. XRD patterns of CuO NPs

On this spectrum we notice a series of diffraction peaks which are surpassed in intensity representing the diffraction peaks of our compound whose positions 2 θ=32.86°, 35.78° ,38.91°, and 48.98°. Corresponding to the diffraction planes (002) (1̄11) (111) and (2̄02). These diffraction peaks correspond to the CuO formation, note that the first four peaks are more intense. It can be noted that all the peaks obtained correspond to the monoclinic phase of the CuO also we can deduce that the prepared powder is pure and does not present other phases nor impurities such as Cu_2O or $Cu(OH)_2$. Moreover, all peaks have a wide profile that we can match with the low grain size.

The crystallite size is calculated using Scherrer's formula for the first three highest peaks.

$$D = \frac{0.9\lambda}{cos\,\theta} \qquad (1)$$

Where D is average grain size, k is the X-ray wavelength (0.154 nm), λ is the wavelength of the incident X-ray (Cu Kα radiation, λ = 1.5418 Å), β is the FWHM (full width at halfmaximum intensity) and θ is the Bragg angle (in radians). The grain size value of the elaborated powder is 30nm which reflects the fact that the powder prepared is nanoscale.

3.2. Morphological studies of CuO nanoparticles

From the SEM images of the CuO samples (Figure. 2), the observed powder has a flower-like structure with good homogeneity and dispersion. Three-dimensional CuO nanoflowers are formed from two-dimensional CuO nanosheets.

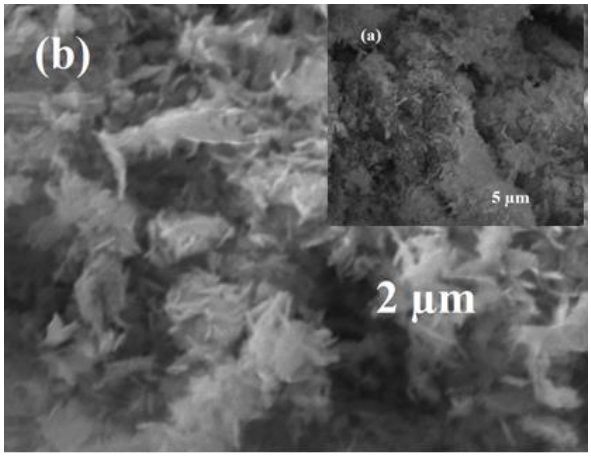

Figure 2. The SEM images of the nano-flower CuO.

3.3. Chemical composition of CuO nanoparticles

In order to detect the elements present in the CuO material, EDS analysis (energy dispersive X-ray analysis) was performed, as shown in Figure 3, which indicates the presence of copper [Cu] and oxygen [O]. No other impurities are detected, see table 1.

Table1: Elemental analysis of CuO NPs.

Element	Weight%	Atomic %
O	16.46	43.90
Cu	83.54	56.10
Total	100	100

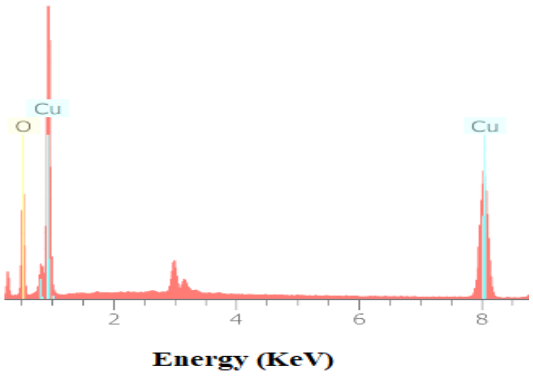

Figure 3. EDS spectrum recorded for CuO NPs

3.4. FTIR Analysis of CuO nanoparticles

The infrared spectra of our samples were recorded on a spectrometer. FTIR Thermo-Nicolet, in the spectral range 400 to 4000 cm^{-1}

Fig. 4 shows the infrared absorption spectrum of the prepared CuO powder at room temperature.

The spectrum shows the presence of three characteristic bands of CuO powder without annealing are located: at 420 cm^{-1}, 495cm^{-1}, and 601cm^{-1}, all these bands can be assigned to the Au mode, Bu mode, and the other Bu mode of CuO, the high frequency mode located at 601 cm^{-1}, is assigned to the elongation of the Cu-O bond along the directions [101], while the peak at 495cm^{-1} can be assigned to the deformation vibrations of the Cu-O bond along the directions [101] [26].

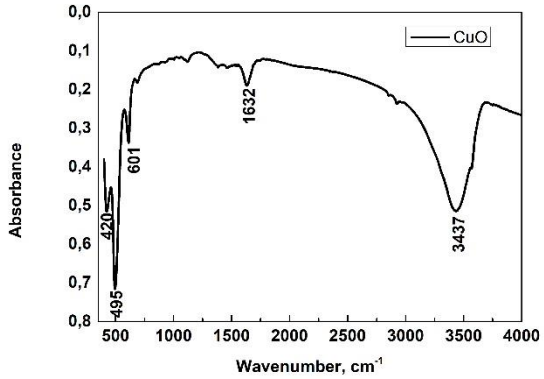

Figure 4. FTIR spectra of CuO NPs in the game 400-4000 cm^{-1}

For the spectrum of the CuO powder no other active infrared mode was observed in the spectral range 605- 600 cm^{-1}, which completely eliminates the existence of another phase like Cu_2O. The two bands located at 1632cm^{-1} and 3437cm^{-1} are attributed respectively to the deformation and elongation vibration of the O-H bond, indicating the presence of water (H_2O). All the values are tabulated in Table 2.

Table2: The main peaks in the FTIR spectrum for CuO nanoparticles and their assignment

Characteristic absorption vibrations cm^{-1}	Functional group
3437	(O-H) Stretching Vibration
1632	O-H Bending Vibration
601	Cu-O Stretching Vibration
495	Cu-O Stretching Vibration
420	Cu-O Stretching Vibration

3.5. Optical properties: UV-visible analysis

Fig. 5 displays the spectrum of UV-vis transmittance that was used to determining the electronic structure and properties of optical absorption of a synthesized sample of CuO. The band gap energy that was estimated around

1.34eV, suggesting that the CuO has a three-dimensional flower like nanostructure possesses, increasing electronic transition and photocatalytic efficiency evaluated by comparing to other structures.

Fig. 5 displays the spectrum of UV-vis transmittance that was used to determine the electronic structure and properties of the optical absorption of a synthesized sample of CuO. The band gap energy was estimated around 1.34eV, by Tauc's formula:

$(\alpha h\nu)^n = \beta(h\nu - Eg)$ (2)

Where α is the absorption coefficient, hν is the photon energy, β is a constant, Eg is the optical band gap and n depends on the type of transition. For n = ½

This band gap value is fully in agreement with the experimental value (1.2 eV), suggesting that the CuO has a three-dimensional flower-like nanostructure possesses which increasing electronic transition and photocatalytic efficiency evaluated by comparing to other structures.

Table3 : Pseudo-first-order kinetic parameters of MB degradation.

Samples	Value			Standard deviation			R^2
	K(min^{-1})	X	E	K(min^{-1})	X	E	
CuO	0.0457	0.2491	0.7493	0.0134	0.0248	0.0154	0.9729

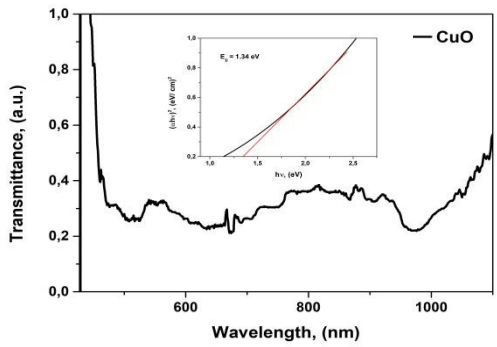

Figure 5. Transmission spectra of CuO NPs

3.6. Photocatalytic activity of CuO nanoparticles

The evolution of the UV-Vis absorption spectra of MB as a function of time in the presence of copper nanoparticles is shown in figure 6. These spectra show a significant decrease of the MB absorption band at 664 as a function of time after the addition of copper, indicating the degradation of MB.

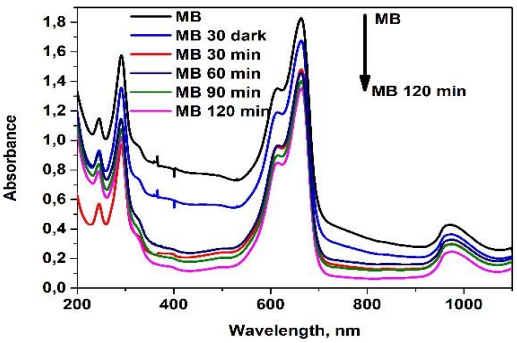

Figure 6. The effect of CuO NPs on the absorption spectra of MB solution for different reaction time under UV light illumination.

3.7. Kinetic studies

In order to examine the mechanism of the degradation process and to provide essential information for the use of copper nanoparticles. Several formalisms are given in the literature to describe the degradation kinetics.

In this work we have adapted a single kinetics model to the pseudo-first order. Figure 7 shows the kinetics of the degradation reaction of methylene blue in Solution, and he calculated kinetic parameters of MB degradation are shown in Table 3, according to the equation [27].

$A = X * exp(-k * t) + E$ (3)

While the unit of (pseudo-) order rate constant k is the inverse of the unit of time used (min^{-1}), X is the amplitude of the process, E is the endpoint, both of them have the same units as the measured quantity A. These results show that copper nanoparticles give a better degradation rate

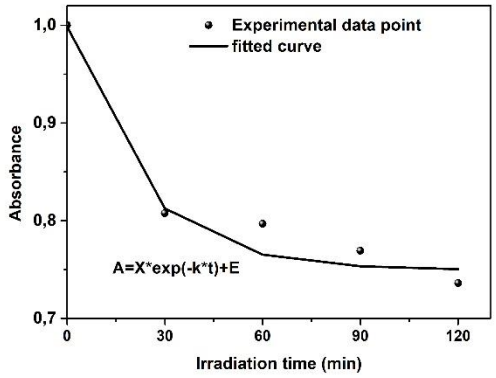

Figure 7. Decolorization kinetics of MB aqueous solutions by CuO NPs without UV light illumination

4. Conclusion

In this work we have developed and characterized copper nanoparticles by the simple chemical method with a yield of 67%, which is a non-cutting and easy to implement method. Finally, we tested these nanoparticles for the degradation of methylene blue in the presence of UV light. The synthesized powders were characterized from a structural and microstructural point of view by X-ray diffraction, SEM, EDS and infrared spectroscopy. Optical characterization was performed by UV-Visible analysis.

The X-ray study identified a monoclinic phase with a good crystalline quality, the average crystallite size is 16.76nm, SEM characterization indicates the formation of CuO nanoflowers in size, while characterization by Fourier transform infrared spectroscopy (FTIR) confirmed the presence of the characteristic bands of copper oxide CuO, indicating the formation of CuO. The study of the optical properties of CuO nanoparticles allowed to estimate the value of the optical gap, of the order of 1.34eV, giving a decrease of the band gap compared to that of massive CuO. Catalytic tests show that the degradation rate of methylene blue at room temperature is 67% after 120 min for a 20 mg of copper. The rate of degradation increases

Acknowledgments

Funding was provided by the General Direction of research and development technologies/ Ministry of Higher Education and Research Sciences DGRSDT/ MESRS, Algeria. The financial support from Abbes Laghrour University of Khenchela (Algeria). The authors would like to thank the National Project Research (PNR) and LASPI²A Laboratory of Khenchela University (Algeria) for their financial support of this research project. The authors thank Pr. Abdecharif Boumaza for FTIR analysis, Laboratoire des Structures, Propriétés et Interactions Inter Atomiques (LASPI2A), Université Abbes Laghrour, 40000 Khenchela, Algeria.

References

[1] B. Purusottam Reddy, K. Sivajee Ganesh, O.M. Hussain, Appl Phys A. 122 (2016)1.
[2] M. Lamri Zeggar, F. Bourfaa, A. Adjimi, M.S. Aida, N. Attaf, IOP Conf. Ser, Mater. Sci. Eng. 108 (2016) 1.
[3] T.J. Richardson, J.L. Slack, M.D. Rubin, Acta. 46 (2001) 2281.
[4] H. Kidowaki, T. Oku, T. Akiyama, J Phys, Conf Ser. 352 (2012) 1.
[5] E.O. Omayio, P.M. Karimi, W.K. Njoroge, F.K. Mugwanga, Int J Thin Film Sci Tec. 2 (2013) 25.
[6] X. Zhang, J. Song, J. Jiao, X. Mei, Solid State Sci. 12 (2010) 1215.
[7] M.R. Johan, M.S.M. Suan, N.L. Hawari, H.A. Ching, Int. J. Electrochem. Sci. 6 (2011) 6094
[8] N. Serin, T. Serin, S. Horzum, Y. Celik, Semicond. Sci. Technol. 20 (2005) 398
[9] W. Siripala, A. Ivanovskaya, T.F. Jaramillo, S.H. Baeck, E.W. McFarland, Sol. Energy Mater. Sol. Cells 77 (2003) 229
[10] H. Yang, J. Ouyang, A. Tang, Y. Xiao, X. Li, X. Dong, Y. Yu, Mater. Res. Bull. 41(2006) 1310
[11] B.J. Wood, H. Wise, R.S. Yolles, J. Catal. 15 (1969) 355
[12] J. Li, L. Liu, Y. Yu, Y. Tang, H. Li, F. Du, Electrochem. Commun. 6 (2004) 940
[13] M. Rabbani, R. Rahimi, M. Bozorgpour, J. Shokraiyan, S.S. Moghaddam, Mater. Lett. (2014), https://doi.org/10.1016/j.matlet.2013.12.095
[14] Y. Zhang, P. Zhu, G. Li, L. Chen, C. Cui, K. Zhang, R. Sun, C. Wong, Mater. Lett. (2018), https://doi.org/10.1016/j.matlet.2017.10.127.
[15] W.Z. Wang, G.H. Wang, X.S. Wang, Y.J. Zhan, Y. K. Liu, and C.L. Zheng, Adv Mater. 14 (2002) 67.
[9] L. Yu, G. Zhang, Y. Wu, X. Bai, and D. Guo, J Crystal Growth. 310 (2008) 3125
[17] K.M. Shrestha, C. M. Sorensen, K. J. Klabunde, J Phys Chem C. 114 (2010) 14368
[18] X. Lü, A. Chen, Y. Luo, P. Lu, Y. Dai, E. Enriquez, P. Dowden, H. Xu, P.G. Kotula, A.K. Azad, D.A. Yarotski, R.P. Prasankumar, A.J. Taylor, J.D. Thompson, Q. Jia, Nano Lett. (2016), https://doi.org/10.1021/Acs.nanolett.6b02454.
[19] J. Li, M. Cui, Z. Guo, Z. Liu, Z. Zhu, Mater. Lett. (2014), https://doi.org/10.1016/j.matlet.2014.05.084.
[20] S. Sonia, S. Poongodi, P. S., Kumar, D. Mangalaraj, N. Ponpandian, C. Viswanathan, Mater Sci Semicond Process 30 (2015) 585.
[21] K. Mageshwari, R. Sathyamoorthy, J. Park, Powder technol. 278 (2015) 150.
[22] S.K. Misra, S. Nuseibeh, A. Dybowska, D. Berhanu, T.D. Tetley, E.V. Jones, Nanotoxicology. 8 (2014) 422.
[23] L. Chen, S. Shet, H. Tang, H. Wang, T. Deutsch, Y. Yan, J. Turner, and M. Al- assim, J Mater Chem. 20 (2010) 6962.
[24] R. Al-Gaashani, S. Radiman, N. Tabet, and A.R. Daud, J Alloys Compd. 509 (2011) 8761.
[25] H. Xu, W. Wang, W. Zhu, J. Phys. Chem. B 110 (2006) 13829
[26] A. Sagadevan Ethira, D. and Joon Kang, Ethiraj and Kang Nanoscale Research Letters. 7 (2012) 70.
[27] G. Lente, Deterministic Kinetics in Chemistry and Systems Biology, 1st ed., Springer, Cham, 2015